Editors' Suggestion

Kondo temperature evaluated from linear conductance in magnetic fields

Rui Sakano*
Faculty of Science and Technology, Keio University, 3-14-1 Hiyoshi, Kohoku-ku, Yokohama 223-8522, Japan

Tokuro Hata
Department of Physics, Tokyo Institute of Technology, 2-12-1 Ookayama, Meguro, Tokyo 152-8551, Japan

Kaiji Motoyama
Department of Physics, Osaka City University, Sumiyoshi-ku, Osaka 558-8585, Japan

Yoshimichi Teratani, Kazuhiko Tsutsumi, and Akira Oguri
Department of Physics, Osaka City University, Sumiyoshi-ku, Osaka 558-8585, Japan
and Nambu Yoichiro Institute of Theoretical and Experimental Physics, Osaka Metropolitan University, Sumiyoshi-ku, Osaka 558-8585, Japan

Tomonori Arakawa
National Institute of Advanced Industrial Science and Technology, National Metrology Institute of Japan, Tsukuba, Ibaraki 305-8563, Japan

Meydi Ferrier and Richard Deblock
Université Paris-Saclay, CNRS, Laboratoire de Physique des Solides, 91405 Orsay, France

Mikio Eto
Faculty of Science and Technology, Keio University, 3-14-1 Hiyoshi, Kohoku-ku, Yokohama 223-8522, Japan

Kensuke Kobayashi
Institute for Physics of Intelligence and Department of Physics, The University of Tokyo, Bunkyo-ku, Tokyo 113-0033, Japan

(Received 17 April 2023; revised 21 August 2023; accepted 30 October 2023; published 21 November 2023)

We theoretically and experimentally study the universal scaling property of the spin-$\frac{1}{2}$ Kondo state in the magnetic field dependence of bias-voltage linear conductance through a quantum dot at low temperatures. We discuss an efficient and reliable procedure to evaluate the Kondo temperature defined at the ground state from experimental or numerical data sets of the magnetic field dependence of the linear conductance or the magnetization of the quantum dot. This procedure is helpful for quantitative comparison of the theory and the experiment, and useful in Kondo-correlated systems where temperature control over a wide range is difficult, such as for cold atoms. We demonstrate its application to experimentally measure electric current through a carbon nanotube quantum dot.

DOI: 10.1103/PhysRevB.108.205147

I. INTRODUCTION

The Kondo effect is a typical many-body phenomenon of electrons in metals and has been thoroughly studied for over 60 years [1,2]. It is a phenomenon in which a localized magnetic moment of a magnetic impurity, or quantum dots, is screened by conduction electrons to form a many-body singlet ground state. Simultaneously, the Kondo resonance state emerges in the impurity or the quantum dot at the Fermi level of the conduction electrons. In quantum dots, the tunneling through the resonance state enhances the electric current between two leads at low temperatures. The Kondo effect in quantum dots has been experimentally observed as an increase of bias-voltage linear conductance with lowering the temperature in dilution refrigerators [3–5]. Recently, the Kondo effect has been intensively investigated in various physical systems, such as dilute magnetic alloys, heavy fermions [1], quantum dots [3–5], cold atoms [6–9], and quark matter [10,11].

A prominent feature of the Kondo effect is the scaling universality in the temperature dependence of physical quantities and their response to external fields at lower energies than a scaling energy. The scaling energy is called the Kondo temperature. At much lower temperatures than the Kondo temperature, the local Fermi liquid describes the properties of the Kondo effect, which is an extension of Landau's Fermi liquid to impurity or quantum dot systems [12,13]. In the local Fermi liquid theory, only one parameter given by the Kondo temperature describes the low-energy state. Namely,

*sakano@keio.jp

the Kondo temperature is the essential quantity to understand the low-energy properties of the Kondo effect.

The Kondo temperature can be deduced from low-energy properties, such as the ground-state value of magnetic susceptibility, the coefficient of the T-linear specific heat, or the width of the Kondo resonance. In experiments, the Kondo temperature is usually determined by the energy scale of the crossover transition between low and high energies. However, it is challenging to specify the crossover transition point, such that it is quantitatively consistent with the theoretically defined Kondo temperature. Evaluation of the Kondo temperature that is quantitatively consistent with theory is the key to exploring the frontier of the local Fermi liquid nature of the many-body state, such as nonlinear current and current due to the Kondo correlation [14–21]. It is also demanded to investigate systems in which the Kondo effect competes with other correlation effects, such as superconductivity and spin-orbit interaction [22–26]. This paper aims to show an efficient and reliable procedure to evaluate the Kondo temperature that is quantitatively consistent with local Fermi liquid theory from a data set of magnetic field dependence of linear conductance through a quantum dot. Our procedure is extendable to magnetic field dependence of other quantities in a variety of Kondo correlated systems.

In 1998, Goldhabar-Gordon *et al.* devised an empirical formula for the temperature dependence of the linear conductance of electric current through a quantum dot connecting to two electric leads [3,4,16,17]. They assume a simple analytic function,

$$G_{\rm emp}(T) = G_0 \left[1 + \left(\frac{T}{\widetilde{T}_{\rm K}^{\rm emp}} \right)^2 \right]^{-s}, \tag{1}$$

as the temperature dependence of the linear conductance. Here, $G_0 = \frac{2e^2}{h} \frac{4\Gamma_L \Gamma_R}{(\Gamma_L+\Gamma_R)^2}$, and the Kondo temperature is empirically determined by $\widetilde{T}_{\rm K}^{\rm emp} = T_{\rm K}^{\rm emp}/\sqrt{2^{1/s}-1}$ so that $G_{\rm emp}(T_{\rm K}^{\rm emp}) = G_0/2$. $\Gamma_L(\Gamma_R)$ is the linewidth due to the electron tunneling between the left (right) lead and the dot, as defined in the next section. The curve fitting to a set of data calculated by the numerical renormalization group (NRG) approach for the spin-$\frac{1}{2}$ Anderson impurity model determines the fitting parameter as $s = 0.22$. Mesoscopic physicists have frequently applied the curve fitting to experimental data to evaluate the Kondo temperature, taking Eq. (1) as the model function and $T_{\rm K}^{\rm emp}$ as the fitting parameter. Kretinin *et al.* showed that this empirical Kondo temperature relates to the Kondo temperature defined in the local Fermi liquid theory $T_{\rm K}$ given in Eq. (8) as

$$T_{\rm K}^{\rm emp} = \eta(U)\, T_{\rm K}, \tag{2}$$

with $\eta(U)$ that depends on the Coulomb interaction U at the dot site [16]. Namely, the empirically evaluated Kondo temperature demands an extra factor to be consistent with the Kondo temperature defined in the local Fermi liquid theory.

In this paper, we theoretically investigate the scaling universality in magnetic field dependence of the linear conductance of a quantum dot, using the numerical renormalization group approach and the Bethe ansatz exact solution. Strong magnetic fields suppress the Kondo effect, as it has also been observed in transport experiments of quantum dots [3–5,27–29]. Exploiting the universal curve of the magnetic-field scaling at $T = 0$, we develop a simple procedure to evaluate the Kondo temperature of the local Fermi liquid theory from magnetic field dependence of the linear conductance, while Goldhabar-Gordon's approach given by Eq. (1) uses the excited state. Then, we examine our procedure for experimental data on electric current measured in a carbon nanotube quantum dot.

There have already been a lot of preceding works on magnetotransport and magnetic properties in the Kondo impurity and the Kondo dot [28–41]. We here develop a way to evaluate the Kondo temperature with the use of the universal curve of the *bias-voltage-linear* magnetoconductance. In our previous work, we evaluated the Kondo temperature using the universal curve of the bias-voltage *bias-voltage-nonlinear* magnetoconductance [20]. This curve fitting of the linear conductance still has the following advantages. The linear conductance is a monotonous function of the applied magnetic field, as seen in this paper, while the nonlinear one is non-monotonous. Naively, the measurement and evaluation of the Kondo temperature for the linear conductance is simpler and easier than that for the nonlinear one in experiments. In particular, the Kondo temperature evaluated from the magnetic field dependence in our approach is quantitatively consistent with the one defined by the linewidth of the quasiparticle in the local Fermi liquid theory. In semiconductor nanodevice experiments, manipulation of the magnetic field is more stable and easy than temperature control. Indeed, it is technically demanding to systematically address the temperature between 1 K and 4 K in dilution refrigerators. In addition, changing temperature could be more challenging in other systems, such as cold atoms. Therefore, our method using magnetic fields is promising for extending the research field of the Kondo physics.

This paper is organized as follows. In Sec. II, we introduce our model of a quantum dot system and explain the calculation of the linear conductance. In Sec. III, we discuss the universal behavior of the Kondo state on the magnetic field dependence of the linear conductance through a quantum dot and our way to estimate the Kondo temperature from the magnetic field dependence. Then, in Sec. III, we demonstrate its application to experimental data measured in a carbon nanotube quantum dot. Finally, in Sec. IV, we summarize the paper.

II. MODEL AND CALCULATION

We introduce the model to describe a quantum dot, where the Kondo state enhances the electric current. We also define the Kondo temperature in the local Fermi liquid theory. Then we show an analytical result of the linear conductance under applied magnetic fields, using the Bethe ansatz exact solution.

A. Model

Let us consider a quantum dot connected to two electric leads, which is described by the spin-$\frac{1}{2}$ Anderson impurity model

$$\mathcal{H}_{\rm A} = \mathcal{H}_{\rm d} + \mathcal{H}_{\rm c} + \mathcal{H}_{\rm T} \tag{3}$$

with

$$\mathcal{H}_{\rm d} = \sum_{\sigma} \epsilon_{\rm d} n_{{\rm d}\sigma} - \mu_{\rm B} B\, m_{\rm d} + U n_{{\rm d}\uparrow} n_{{\rm d}\downarrow}, \tag{4}$$

$$\mathcal{H}_{\rm c} = \sum_{\gamma\sigma} \int_{-D}^{D} d\varepsilon\, \varepsilon c^{\dagger}_{\varepsilon\gamma\sigma} c_{\varepsilon\gamma\sigma}, \tag{5}$$

$$\mathcal{H}_{\rm T} = \sum_{\gamma\sigma} (v_{\gamma} d^{\dagger}_{\sigma} \psi_{\gamma\sigma} + v^{*}_{\gamma} \psi^{\dagger}_{\gamma\sigma} d_{\sigma}). \tag{6}$$

$\mathcal{H}_{\rm d}$ represents that electrons interact with each other by the Coulomb interaction U at the energy level of the quantum dot $\epsilon_{\rm d}$ under the applied magnetic field B. $n_{{\rm d}\sigma}(:=d^{\dagger}_{\sigma} d_{\sigma})$ is the operator of the electron occupation at the dot site and $m_{\rm d}(:=n_{{\rm d}\uparrow} - n_{{\rm d}\downarrow})$ is the magnetization, where the operator d_{σ} annihilates an electron with energy $\epsilon_{\rm d}$ and spin $\sigma = \uparrow, \downarrow$ at the dot site. $\mu_{\rm B}$ is the Bohr magneton and we set the g factor as $g = 2$. $\mathcal{H}_{\rm c}$ represents the conduction electrons in the left lead $\gamma = L$ and the right lead $\gamma = R$ with half width of the conduction band D. The operator $c_{\varepsilon\gamma\sigma}$ annihilates an electron with energy ε and spin σ in the lead γ, and satisfies with the anticommutation relation $\{c^{\dagger}_{\varepsilon\gamma\sigma}, c_{\varepsilon'\gamma'\sigma'}\} = \delta(\varepsilon - \varepsilon')\, \delta_{\gamma\gamma'}\, \delta_{\sigma\sigma'}$. $\mathcal{H}_{\rm T}$ represents electron tunneling between the dot and the leads via the tunneling matrix v_{γ} and $\psi_{\gamma\sigma} := \sqrt{\rho_{\rm c}} \int_{-D}^{D} d\varepsilon\, c_{\varepsilon\gamma\sigma}$ with $\rho_{\rm c}$ the density of states of the conduction electrons. The linewidth of the dot level due to the electron tunneling is

$$\Delta := \tfrac{1}{2}(\Gamma_L + \Gamma_R), \quad \Gamma_{\gamma} := 2\pi \rho_{\rm c} v^{2}_{\gamma}. \tag{7}$$

We measure $\epsilon_{\rm d}$ and ε from the chemical potential of the leads at equilibrium $\mu_L = \mu_R = 0$. We use $\hbar = k_{\rm B} = 1$ throughout this paper.

In this paper, we define the Kondo temperature by $\widetilde{\Delta}$ the renormalized linewidth of the quasiparticle of the local Fermi liquid in the form

$$T_{\rm K} := \frac{\pi \widetilde{\Delta}}{4}. \tag{8}$$

The linewidth of the quasiparticle is given by the wave function renormalization factor z as $\widetilde{\Delta} = z\Delta$ in the microscopic theory. The renormalization factor

$$z = \left[1 - \left. \frac{\partial \Sigma^{\rm r}_{{\rm d}\sigma}(\omega)}{\partial \omega} \right|_{\omega=0} \right]^{-1} \tag{9}$$

is given by $\Sigma^{\rm r}_{{\rm d}\sigma}(\omega)$ the self-energy of the retarded Green's function for the electrons in the dot at absolute zero. We note that the Kondo temperature is also determined by the spin susceptibility $\chi_{\rm s} = \mu_{\rm B} \partial \langle m_{\rm d} \rangle / \partial B|_{B=0,T=0}$ or the T-linear specific heat coefficient $\gamma_{\rm d} = \lim_{T\to 0} C(T)/T$. Here, $m_{\rm d} = n_{{\rm d}\uparrow} - n_{{\rm d}\downarrow}$ is the magnetization at the dot, and $C(T)$ is the specific heat. This definition is consistent with Eq. (8) in the Kondo regime: $\chi_{\rm s}/{\mu_{\rm B}}^2 = (6/\pi^2)\gamma_{\rm d} = T_{\rm K}^{-1}$ in the Kondo limit.

B. Linear conductance

The linear conductance of the electric current through the quantum dot with applied bias voltages between leads L and R at absolute zero in the magnetic fields is given in the form

$$G = \frac{G_0}{2} \sum_{\sigma} \sin^2 \delta_{\sigma}. \tag{10}$$

The conductance is given only by the phase shift δ_{σ} that describes the Kondo ground state. Friedel's sum rule relates the phase shift δ_{σ} to the number of the electrons at the dot as $\delta_{\sigma} = \pi \langle n_{{\rm d}\sigma} \rangle$. At the half-filling point $\epsilon_{\rm d} = -U/2$, the conductance is given by the magnetization at the dot $\langle m_{\rm d} \rangle$ in a simple form [37],

$$G = G_0 \cos^2 \left(\frac{\pi}{2} \langle m_{\rm d} \rangle \right), \tag{11}$$

because the particle-hole symmetry fixes the total number of the electrons at the dot site as $\langle n_{\rm d} \rangle = 1$ with $n_{\rm d} = n_{{\rm d}\uparrow} + n_{{\rm d}\downarrow}$. We use the numerical renormalization group approach and the Bethe ansatz exact solution (BAES) to calculate the electron occupation and the magnetization at the dot.

Next, we consider extending the applicability of Eq. (11) to the Kondo regime where $\Delta \ll -\epsilon_{\rm d}$ and $\Delta \ll U + \epsilon_{\rm d}$. The first inequality means that either one or two electrons occupy the dot, while the second inequality excludes two-electron occupation. The charge fluctuation is drastically suppressed as $\chi_{\rm c}/\chi_{\rm s} \ll 1$, with $\chi_{\rm c} = -\frac{\partial \langle n_{\rm d} \rangle}{\partial \epsilon_{\rm d}}$ the charge susceptibility. This results in the total number of electrons at the dot site being locked at $\langle n_{\rm d} \rangle \simeq 1.0$ in the Kondo regime. Therefore, the conductance in the Kondo regime is given in the form $G \simeq G_0 \cos^2(\frac{\pi}{2} \langle m_{\rm d} \rangle)$ with Eq. (11).

In the Kondo regime we have the exact solution for the Kondo model (see Appendix A) [42]. The magnetic field dependence of the magnetization is given in simple series and integral as

$$\langle m_{\rm d} \rangle = \sum_{n=0}^{\infty} \frac{(-1)^n}{n!} \left(\frac{\pi}{4} \right)^n (2n+1)^{n-\frac{1}{2}} \left(\frac{\mu_{\rm B} B}{T_{\rm K}} \right)^{2n+1} \tag{12}$$

for $\mu_{\rm B} B \leqslant \sqrt{2/(e\pi)}\, T_{\rm K}$, and

$$\langle m_{\rm d} \rangle = 1 - \pi^{-\frac{3}{2}} \int_0^{\infty} dx\, \sin(\pi x) \frac{\Gamma\left(x + \frac{1}{2}\right)}{x^{x+1}} \left(\frac{2}{\pi} \right)^x \left(\frac{\mu_{\rm B} B}{T_{\rm K}} \right)^{-2x} \tag{13}$$

for $\mu_{\rm B} B > \sqrt{2/(e\pi)}\, T_{\rm K}$. Here, we note that $\sqrt{2/(e\pi)} = 0.4839\ldots$.

Using this exact result, we also derive the asymptotic form of the conductance for small and large magnetic fields. For small magnetic fields $\mu_{\rm B} B \ll T_{\rm K}$, the linear conductance is given up to the leading B-dependent term in the form [33,36]

$$\begin{aligned} G(B) &= G_0 \left[1 - \frac{\pi^2}{4} \left(\frac{\chi_{\rm s}}{\mu_{\rm B}} B \right)^2 \right] + \mathcal{O}\left[\left(\frac{\chi_{\rm s}}{\mu_{\rm B}} B \right)^4 \right] \\ &= G_0 \left[1 - \frac{\pi^2}{4} \left(\frac{\mu_{\rm B} B}{T_{\rm K}} \right)^2 \right] + \mathcal{O}\left[\left(\frac{\mu_{\rm B} B}{T_{\rm K}} \right)^4 \right]. \end{aligned} \tag{14}$$

For large fields $\mu_{\rm B} B \gg T_{\rm K}$, the conductance up to the leading B dependence is given in the form

$$G(B) \sim G_0 \frac{\pi^2}{16} \left[\ln \left(\frac{\mu_{\rm B} B}{\sqrt{2/(e\pi)}\, T_{\rm K}} \right) \right]^{-2}. \tag{15}$$

III. RESULTS AND DISCUSSION

We theoretically discuss the universal scaling property of the linear magnetoconductance. Then, using the universal

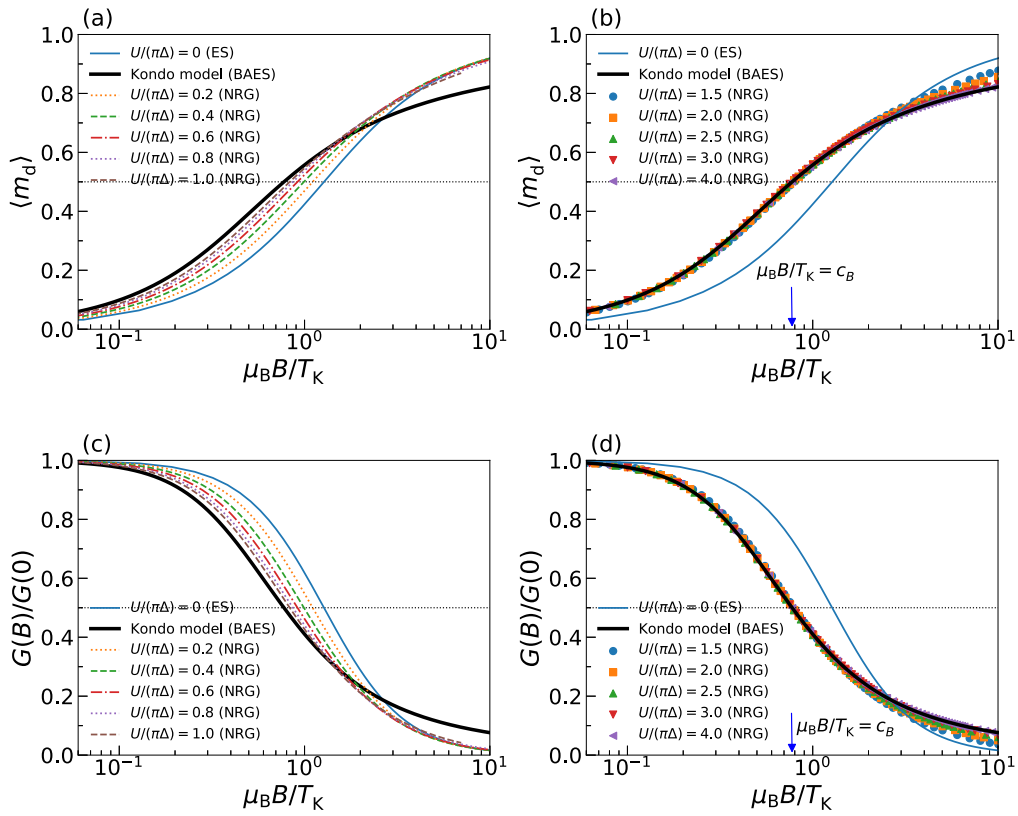

FIG. 1. Magnetization $\langle m_d \rangle$ at particle-hole symmetric point ($\epsilon_d = -U/2$) as a function of magnetic field B at absolute zero for (a) small $U/(\pi\Gamma)(\leqslant 1)$ and (b) large $U/(\pi\Gamma)(\leqslant 1.5)$. The resulting linear conductance G for (c) small $U/(\pi\Gamma)(\leqslant 1)$ and (d) large $U/(\pi\Gamma)(\leqslant 1.5)$. The broken lines and the data points are calculated by the NRG approach. The thin (blue) solid lines are the conductance at absolute zero for the noninteracting limit $U = 0$, which are calculated by the exact solution (ES). The thick solid (black) lines are the conductance for the Kondo limit ($U \gg \Gamma$), which are calculated by the Bethe ansatz exact solution. In this figure, we use the Kondo temperature T_K of the local Fermi liquid theory, given by Eq. (8) at $B = 0$. The arrow in (b) and (d) indicates the magnetic field at which the conductance and the magnetization takes half of the zero field value.

scaling property, we devise a procedure to evaluate the Kondo temperature. We finally demonstrate its application to experimental data of conductance of a carbon nanotube quantum dot.

A. Universal scaling of conductance under magnetic field

We show the magnetization and the linear conductance as a function of the applied magnetic field B at the half-filling point $\epsilon_d = -U/2$ and $T = 0$ in Fig. 1. We used the numerical renormalization group approach for finite U's, the exact result for the noninteracting limit $U = 0$, and the Bethe ansatz exact solution for the Kondo model $U \gg \Delta$ to calculate the quantities. The magnetic field is scaled by the Kondo temperature determined by Eq. (8) at the zero field $B = 0$ for each strength of interaction U, to investigate the universal scaling properties of the Kondo effect.

For a small Coulomb interaction $U/(\pi\Delta) \leqslant 1$, the curve of the magnetic field dependence of the magnetization and the conductance continuously transits between the noninteracting limit and the Kondo limit, as seen in Figs. 1(a) and 1(c). The data points of the magnetic field dependence of the magnetization and the conductance for a large Coulomb interaction $U/(\pi\Delta) \geqslant 1.5$ collapse to a single curve that is given by the Kondo model for $\mu_B B < T_K$ as seen in Figs. 1(b) and 1(d), because of the Kondo universal scaling property. However, for large magnetic fields $\mu_B B > T_K$, the spin fluctuation becomes less pronounced, and the data points consequently deviate from the curve of the Kondo model to the curve for the noninteracting limit $U/(\pi\Delta) = 0$.

Let us consider a procedure to evaluate the Kondo temperature from a measurement of the magnetic field dependence of the linear conductance. As seen in Figs. 1(b) and 1(d), the magnetic field $\bar{B}$ at which the conductance takes the half value of the zero-field value $G(\bar{B}) = G(0)/2$ stays on the universal $\mu_B B/T_K$ scaling curve. Therefore, at this point, the universal function gives the following relationship between the magnetic field $\bar{B}$ and the Kondo temperature:

$$\tfrac{1}{2} g \mu_B \bar{B} = c_B T_K. \tag{16}$$

Here, we reinserted the g factor. We numerically calculate the coefficient c_B using the exact solution for the Kondo model given by Eq. (13) with three significant figures as

$$c_B = 0.774. \tag{17}$$

Our idea is to exploit the relation given by Eq. (16) to efficiently and reliably evaluate the Kondo temperature from a data set of magnetic field dependence of the measured

conductance in the Kondo regime. We apply Eq. (16) to an experimental data set in Sec. III C and demonstrate evaluation of the Kondo temperature. We note that the magnetization at $B = \bar{B}$ also takes half of the value at the fully polarized limit $\langle m_{\rm d}\rangle|_{B\to\infty} = 1$ as

$$\langle m_{\rm d}\rangle|_{B=\bar{B}} = \tfrac{1}{2} \tag{18}$$

for large U as seen in Fig. 1(b). This relation of the magnetization is useful to evaluate the Kondo temperature of systems in which conductance is challenging to be observed, for example, the Kondo effect in cold atoms [6,7,9].

B. Empirical formula for magnetic field dependent conductance

We also present an empirical formula for the magnetic field dependence of the linear conductance similar to the temperature dependence given in Eq. (1). We introduce a formula of magnetic-field dependence of the linear conductance that takes a similar form to the temperature dependence given in Eq. (1), as

$$G^B_{\rm emp}(B) = G_0\left[1 + \left(\frac{B}{\widetilde{B}^{\rm emp}}\right)^2\right]^{-t}. \tag{19}$$

Because we set that the empirical formula takes half of the zero field value at $B = \bar{B}$ as $G^B_{\rm emp}(\bar{B}) = G_0/2$, the Kondo temperature relates to $\widetilde{B}^{\rm emp} = \bar{B}/\sqrt{2^{1/t}-1}$ via Eq. (16). We numerically determine the value of the fitting parameter t as

$$t = 0.498, \tag{20}$$

using the least squares fitting to the universal part ($\mu_{\rm B}B < T_{\rm K}$) of the conductance curve of the spin-$\frac{1}{2}$ Kondo model: We here prepared 2000 data samples of the conductance for equally spaced magnetic fields from $\mu_{\rm B}B = 0$ to $T_{\rm K}$, using the exact solution of the spin-$\frac{1}{2}$ Kondo model. We note that the parameter t is independent of the gate voltage as long as the system is in the Kondo regime or the Kondo plateau in which the charge fluctuation is suppressed $\langle n_{\rm d}\rangle \simeq 1.0$.

We compare the obtained empirical conductance with the exact solution of the Kondo model in Fig. 2. Indeed, the empirical equation and the exact solution agree well at magnetic fields below the Kondo temperature $\mu_{\rm B}B < T_{\rm K}$ while two curves gradually deviate from each other at the higher fields $\mu_{\rm B}B \gtrsim 2T_{\rm K}$.

The empirical formula asymptotically behaves at low fields $\mu_{\rm B}B \ll T_{\rm K}$ as

$$\begin{aligned} G^B_{\rm emp}(B) &= G_0\left[1 - \frac{t(2^{1/t}-1)}{c_B^2}\left(\frac{\mu_{\rm B}B}{T_{\rm K}}\right)^2\right] + \mathcal{O}\left[\left(\frac{\mu_{\rm B}B}{T_{\rm K}}\right)^4\right] \\ &= G_0\left[1 - 2.51\times\left(\frac{\mu_{\rm B}B}{T_{\rm K}}\right)^2\right] + \mathcal{O}\left[\left(\frac{\mu_{\rm B}B}{T_{\rm K}}\right)^4\right]. \end{aligned} \tag{21}$$

This asymptotic form of the empirical formula agrees reasonably with the exact one given in Eq. (14) since $\pi^2/4 = 2.467\ldots$. At high magnetic fields $\mu_{\rm B}B \gg T_{\rm K}$, the empirical formula asymptotically behaves as

$$\begin{aligned} G^B_{\rm emp}(B) &\sim G_0\left(\frac{2^{1/t}-1}{c_B^2}\right)^{-t}\left(\frac{\mu_{\rm B}B}{T_{\rm K}}\right)^{-2t} \\ &= 0.447\times G_0\left(\frac{\mu_{\rm B}B}{T_{\rm K}}\right)^{-1.02}. \end{aligned} \tag{22}$$

This is not consistent with the exact asymptotic form given in Eq. (15). This tendency is clearly seen in Fig. 2 at magnetic fields of $\mu_{\rm B}B \sim 10T_{\rm K}$, where the deviation of the empirical formula from the exact one gradually develops. Nevertheless, the empirical formula has a practical merit as it is a simple function and agrees reasonably well at $\mu_{\rm B}B \lesssim 2T_{\rm K}$ with the exact result for which some extra calculations are needed to obtain the conductance from Eqs. (11)–(13).

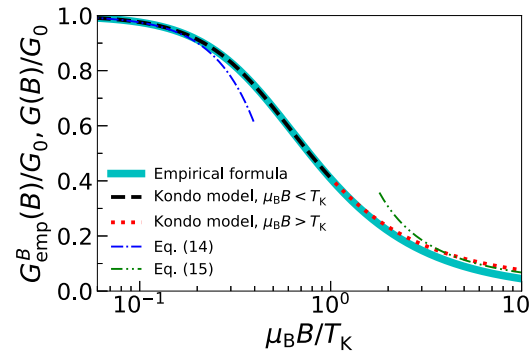

FIG. 2. The linear conductance calculated by the empirical formula for the magnetic field dependence, given in Eq. (19) (the solid line), and comparison with that of the exact solution of the Kondo model (dashed line for $\mu_{\rm B}B < T_K$ and dotted line for $\mu_{\rm B}B > T_K$). The parameter t of the empirical formula is determined to fit the universal part ($\mu_{\rm B}B < T_{\rm K}$) given by the exact solution. The dashed-dotted line and the dashed double-dotted line are asymptotes given by Eq. (14) for $\mu_{\rm B}B \ll T_{\rm K}$ and Eq. (15) for $\mu_{\rm B}B \gg T_{\rm K}$, respectively.

We exploit the magnetic field dependence of the ground state to estimate the Kondo temperature while Goldhaber-Gordon uses the temperature dependence of the excited states. In the next section, we apply our method given in Eq. (16) and Goldhaber-Gordon's empirical formula to experimental data to evaluate the Kondo temperatures. Then, we compare the results obtained by the two different procedures. In our experiments, we estimate the interaction strength to be $2 \lesssim \frac{U}{\pi\Delta} \lesssim 3$ from observation of the Coulomb diamonds. Correspondingly, we adopt $\eta(U) = 1.1$ following the one estimated in the experiment by Kretinin *et al.* [16]. Then, the Kondo temperatures estimated by the two methods are consistent in our experiments.

C. Application to experimental data

We demonstrate an application of Eq. (16) to experimental data of conductance measured in a carbon nanotube quantum dot connected to two aluminum leads in a dilution refrigerator [18–20,25] to evaluate the Kondo temperature of the dot. We show the linear conductance as a function of the gate voltage corresponding to the dot level with varying applied magnetic field from 0.08 T to 4.08 T at 16 mK in Fig. 3(a), and for

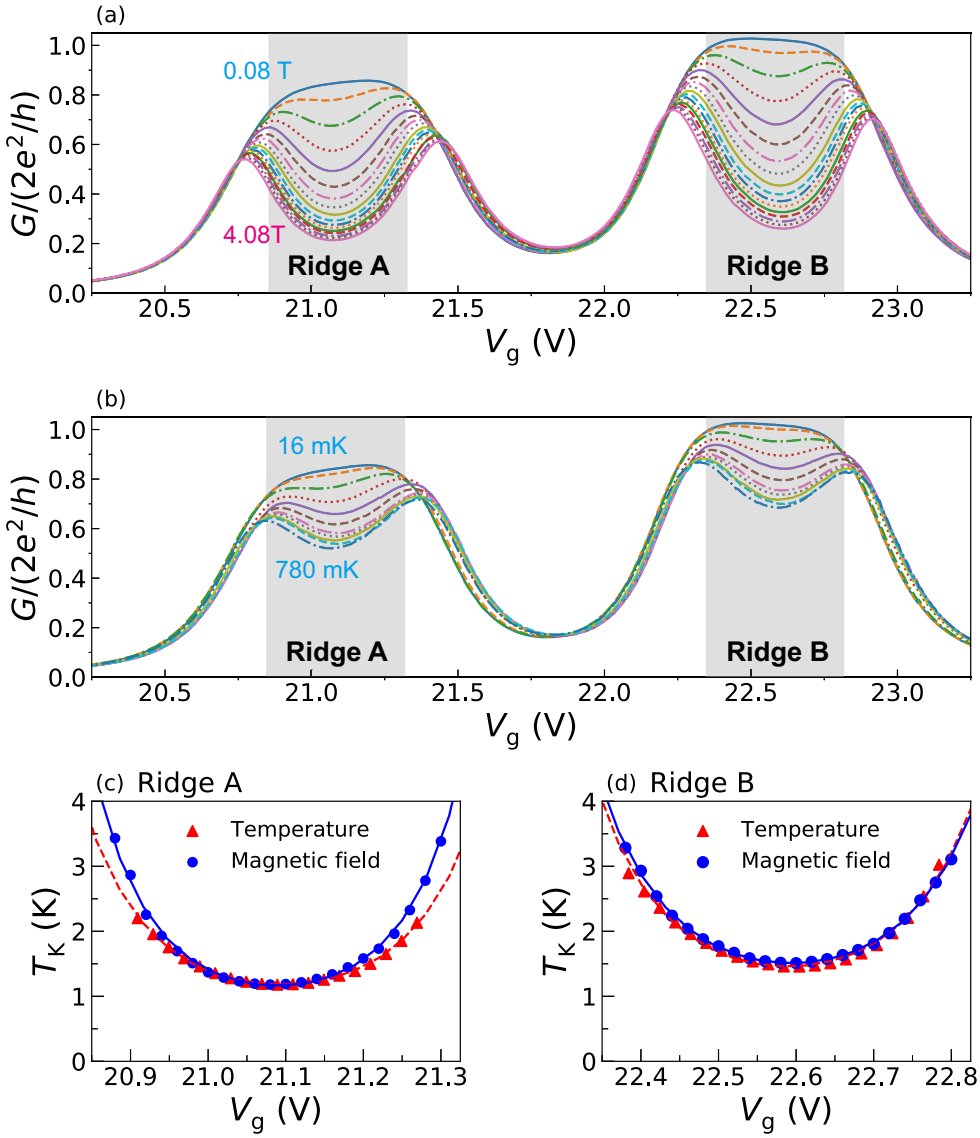

FIG. 3. Experimentally measured linear conductance G as a function of gate voltage V_g (a) at 16 mK with magnetic fields from 0.08 T to 4.08 T in 0.25 T steps, and (b) at 0.08 T and for several temperatures (16, 80, 180, 280, 380, 480, 580, 630, 680, 730, and 780 mK). The left conductance ridge around $V_g \sim 21.1$ V and right one around $V_g \sim 22.6$ V are labeled as Ridges A and B, respectively. (c and d) Evaluated Kondo temperature T_K for Ridges A and B, respectively. The Kondo temperature is evaluated by using Eq. (16) for the magnetic field dependence of the conductance (●) and the empirical formula given in Eq. (1) (▲) with $\eta(U) = 1.1$ for the temperature dependence of the conductance. The solid and dashed lines are the fitting curves given by Eq. (B1).

temperatures from 16 mK to 780 mK at 0.08 T in Fig. 3(b). A small finite magnetic field remains even at the minimum magnetic field to kill the superconductivity in the aluminum leads. There are two regions in which the spin Kondo effect enhances the conductance around $V_g \sim 21.1$ V and $V_g \sim 22.6$ V in Figs. 3(a) and 3(b). We refer to these regions as Ridge A and Ridge B for the convenience of discussion. The value of the gate voltage for each ridge corresponds to the dot level through $\epsilon_d = \alpha U(V_g - V_0)$ with the α factor that presents the lever arm to tune the dot level.

As seen in Fig. 3(a), an increase in the magnetic field suppresses the Kondo effect and it results in decreases in the conductance in both Ridges A and B. Because of the shapes of Ridges A and B, it is found that the Kondo effect fully grows the conductance at the lowest magnetic field in the experiment. Thus, the Kondo effect in both ridges developed enough even at a nonzero small field $B = 0.08$ T, and we consider that the conductance reaches the value of the low-temperature limit G_0. The height of the ridges also turns out that the lead-dot connection is almost symmetric $\Gamma_L \simeq \Gamma_R$ in Ridge B while it is asymmetric $\Gamma_L \neq \Gamma_R$ in Ridge A.

Here, let us evaluate the Kondo temperature of the two ridges to the experimental data of the magnetic field dependence of the linear conductance shown in Fig. 3(a). Specifically, we estimated $\bar{B}$ by applying linear interpolation to the two magnetic-field B points that give the conductance $G(B) \simeq G(B_0 = 0.08\ \text{T})/2$ to determine the Kondo temperature through Eq. (16). We also carried out this procedure for

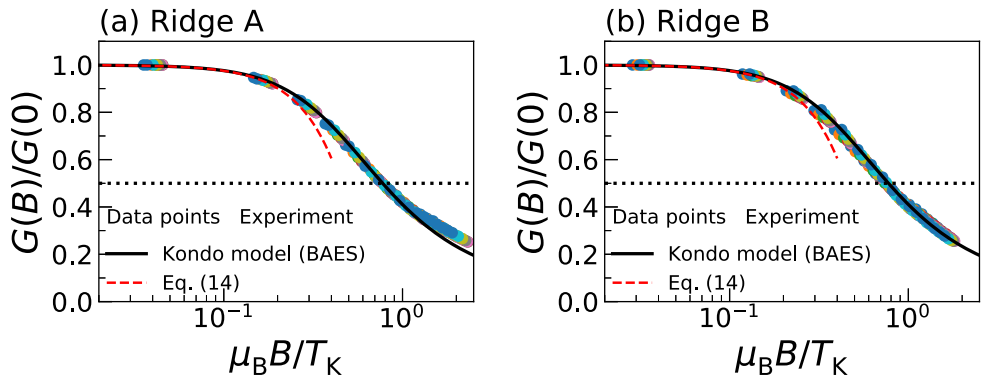

FIG. 4. The linear conductance as a function of the applied magnetic field scaled by the Kondo temperature for several choices of gate voltage V_g corresponding to the Kondo regime. (a) Ridge A with an asymmetric lead-dot connection and (b) Ridge B with a symmetric lead-dot connection. The magnetic field is scaled by the Kondo temperature given in Fig. 3. The solid line is the conductance calculated by the Bethe ansatz exact solution for the Kondo model, which is normalized by the value at zero fields $B = 0$, $G(0) = G_0$. The data points are the experimentally observed conductance (a) for V_g from 20.98 V to 21.18 V in 0.02 V steps in Ridge A and (b) for V_g from 22.48 V to 22.68 V in 0.02 V steps in Ridge B. The experimental conductance is normalized by its value at the lowest field, 0.08T, instead of its zero field value. The values of the Kondo temperature, determined by the magnetic field dependence for each gate voltage, are used. The dashed lines are the formula for the low fields, given by Eq. (14).

several gate voltages in the Kondo regime, for both Ridges A and B shown in Fig. 3(a). We take the g factor of our carbon nanotube quantum dot as $g = 2$ similarly to this theoretical analysis so far [43]. We plot the obtained values of the Kondo temperature T_K as functions of the gate voltage V_g in Ridges A and B in Figs. 3(c) and 3(d), respectively. For comparison, we also evaluate the Kondo temperature from the temperature dependence of the conductance shown in Fig. 3(b) by using the empirical formula given in Eq. (1). The results are also plotted in Figs. 3(c) and 3(d). We here use Eq. (2) and take $\eta(U) = 1.1$ in both Ridges A and B to compare the empirical Kondo temperature $T_K^{\rm emp}$ to the Kondo temperature evaluated from the ground state T_K, similarly to Kretinin *et al.* [16]. As seen in Figs. 3(c) and 3(d), the Kondo temperatures that are evaluated in the two different ways agree very well in both ridges.

Finally, we also examine the universal scaling property in magnetic field dependence of the linear conductance to test the validity of the evaluation of the Kondo temperature in our procedure. The linear conductance as a function of the magnetic field scaled by the Kondo temperature in Ridges A and B are plotted in Figs. 4(a) and 4(b), respectively. In the figure, we scale the magnetic field by the Kondo temperature evaluated by Eq. (16) for each V_g. We find that, for smaller magnetic fields than the Kondo temperature $\mu_B B \lesssim T_K$, the universal scaling property works very well in both ridges. This universal scaling is observed not only at the center of the ridge but also on a broader range of V_g from 20.98 V to 21.18 V for Ridge A, and from 22.48 V to 22.68 V for Ridge B, where the charge fluctuation is suppressed as $\langle n_d \rangle \simeq 1.0$ and $\chi_c/\chi_s \ll 1$. We here conclude that our procedure to evaluate the Kondo temperature from the magnetic field dependence works very well. We note that outside of the gate voltage range shown in Figs. 4(a) and 4(b), the charge fluctuation becomes larger and the scaling universality is gradually broken. We also reported that the universal T/T_K scaling of the conductance works very well in the Kondo plateau of Ridge B, in the supplemental information of Ref. [18].

We examined universal scaling on magnetic field dependence of the nonlinear conductance in Ridge B with the symmetric lead-dot connection $\Gamma_L = \Gamma_R$ in our previous paper [20]. The universal scaling curve of the nonlinear conductance is given in an intricate form of the lead-dot connections Γ_α [44]. However, the linear conductance depends on the asymmetry of the lead-dot connections only through the allover coefficient G_0 that the zero field value determines as $G_0 = G(0)$. This enables one to eliminate the asymmetry of the lead-dot connections from the universal curve of the linear conductance, as seen in the discussion so far. Thus, the universal curve of the linear conductance is less demanding, and our procedure is suited to evaluating the Kondo temperature.

IV. SUMMARY

We have investigated a universal scaling property of the bias-voltage linear response to the applied magnetic field in a quantum dot, using the exact solution for the spin-$\frac{1}{2}$ Kondo model and the numerical renormalization group approach for the spin-$\frac{1}{2}$ Anderson impurity model. Then, we showed a procedure to estimate the Kondo temperature for experimental data sets using the universal curve of the magnetic field dependence of the linear conductance derived by the Bethe ansatz exact solution of the spin-$\frac{1}{2}$ Kondo model. We also demonstrate the application of our procedure to experimental data of linear conductance through a carbon nanotube quantum dot connected to two aluminum leads.

An advantage of our procedure to evaluate the Kondo temperature is that it is applicable to systems in which the temperature is difficult to control, such as ultracold atoms. Although conductance is challenging to observe in cold atom systems, the universal magnetic field dependence of the magnetization can be used to estimate the Kondo temperature as in

the linear conductance. Furthermore, the magnetic field can be varied on a broader energy range with keeping the system stable compared with the system temperature in semiconductor systems. Temperature can also be tuned in a broader energy range in principle, but the thermal cycle with a large temperature range usually gives rise to some changes in system parameters. As seen in our experiment, the applied magnetic field is often varied with a broader energy range than the temperature.

In the paper, the g factor has been fixed at $g = 2$. However, in some actual systems, the g factor is unknown. The g factor can be determined by estimating the Kondo temperature in addition to the magnetic field dependence in other ways. For example, we can estimate $\bar{B}$ from magnetic field dependence of conductance and the Kondo temperature from temperature dependence. Then, we can estimate the g factor by using Eq. (16).

We can also extend this method to determine the Kondo temperature of systems with orbital degeneracy. However, we need to carefully introduce the arrangement of orbitals into the model, because the response of orbitals to applied magnetic fields depends much on materials.

ACKNOWLEDGMENTS

This work was partially supported by JSPS KAKENHI Grants No. JP18K03495, No. JP18J10205, No. JP19H00656, No. JP19H05826, No. JP19K14630, No. JP21K03415, No. JP22H01964, No. JP26220711, No. JP23K03284, and No. JP20K03807; JST CREST Grant No. JPMJCR1876; and the French program ANR JETS (Grant No. ANR-16-CE30-0029-01). K.M. was supported by JST Establishment of University Fellowships towards the Creation of Science Technology Innovation Grant No. JPMJFS2138.

APPENDIX A: KONDO MODEL

We decompose the conduction electrons in left and right leads in the Anderson impurity model (3) to the connected and disconnected electrons to the dot as

$$c_{\varepsilon\sigma} = \frac{v_L}{v} c_{\varepsilon L\sigma} + \frac{v_R}{v} c_{\varepsilon R\sigma}, \tag{A1}$$

$$\bar{c}_{\varepsilon\sigma} = -\frac{v_R^*}{v} c_{\varepsilon L\sigma} + \frac{v_L^*}{v} c_{\varepsilon R\sigma}, \tag{A2}$$

with $v = \sqrt{|v_L|^2 + |v_R|^2}$. This unitary transformation rewrites the electron tunneling and conduction electron parts of the Hamiltonian as

$$\mathcal{H}_{\rm c} = \sum_\sigma \int_{-D}^{D} d\varepsilon\, \varepsilon (c_{\varepsilon\sigma}^\dagger c_{\varepsilon\sigma} + \bar{c}_{\varepsilon\sigma}^\dagger \bar{c}_{\varepsilon\sigma}), \tag{A3}$$

$$\mathcal{H}_{\rm T} = \sum_\sigma v (d_\sigma^\dagger \psi_\sigma + \psi_\sigma^\dagger d_\sigma) \tag{A4}$$

with $\psi_\sigma = \int_{-D}^{D} d\varepsilon \sqrt{\rho_{\rm c}} c_{\varepsilon\sigma}$. Thus, the disconnected state does not contribute to the dot state and is ignored. By applying the Schriefer-Wolf transformation to the Anderson impurity model with $U \gg \Delta$ and $\langle n_{\rm d}\rangle \sim 1$ [45], we get the Kondo model

$$\mathcal{H}_{\rm K} = \sum_\sigma \int_{-D}^{D} d\varepsilon\, \varepsilon\, c_{\varepsilon\sigma}^\dagger c_{\varepsilon\sigma} + J_{\rm K} \sum_{\sigma\sigma'} \frac{1}{2} \psi_\sigma^\dagger \boldsymbol{\sigma}_{\sigma\sigma'} \psi_{\sigma'} \cdot \boldsymbol{S}_{\rm d} - \frac{1}{2} g\mu_{\rm B} B S_{\rm d}^z \tag{A5}$$

with an antiferromagnetic exchange interaction

$$J_{\rm K} = -2v^2 \frac{U}{\epsilon_{\rm d}(\epsilon_{\rm d} + U)} > 0. \tag{A6}$$

Here, $\boldsymbol{\sigma}_{\sigma\sigma'}$ is the Pauli spin matrix, $\boldsymbol{S}_{\rm d}$ is the spin operator at the dot site, and $S_{\rm d}^z$ is the z component of $\boldsymbol{S}_{\rm d}$.

We calculate the magnetization at the dot site $\langle m_{\rm d}\rangle$ using the Bethe ansatz exact solution of this Kondo model in this paper.

APPENDIX B: FITTING FUNCTION OF FIGS. 3(c) AND 3(d)

We use an exponential function with a quadratic as the exponent,

$$F_{\rm fitting}(V_{\rm g}) = \exp\left[c_2 V_{\rm g}^2 + c_1 V_{\rm g} + c_0\right], \tag{B1}$$

as the fitting curve for the gate-voltage dependence of the Kondo temperature. Here, c_0, c_1, and c_2 are the fitting parameters. This function is chosen to be consistent with the asymptotic form of the gate-voltage dependence of the Kondo temperature derived by the scaling analysis [46]. As seen in Figs. 3(c) and 3(d), the curve given by Eq. (B1) fits the evaluated Kondo temperatures very well. Therefore, the gate voltage dependence of the evaluated Kondo temperature via Eq. (16) agrees with the asymptotic behavior that is theoretically expected. We note that, in principle, U and Δ can be deduced from the fitting parameters for systems with large Coulomb interaction $\frac{U}{\pi\Delta} \gtrsim 3$. However, the error of the fitting parameters becomes large because the Kondo temperature is given in the exponential form and deduced interaction is small, $2 \lesssim \frac{U}{\pi\Delta} \lesssim 3$.

[1] A. C. Hewson, *The Kondo Problem to Heavy Fermions*, Cambridge Studies in Magnetism (Cambridge University Press, Cambridge, 1993).

[2] J. Kondo, in *The Physics of Dilute Magnetic Alloys*, edited by S. Koikegami, K. Odagiri, K. Yamaji, and T. Yanagisawa (Cambridge University Press, Cambridge, 2012).

[3] D. Goldhaber-Gordon, H. Shtrikman, D. Mahalu, D. Abusch-Magder, U. Meirav, and M. A. Kastner, Kondo effect in a single-electron transistor, Nature (London) **391**, 156 (1998).

[4] D. Goldhaber-Gordon, J. Göres, M. A. Kastner, H. Shtrikman, D. Mahalu, and U. Meirav, From the Kondo regime to the mixed-valence regime in a single-electron transistor, Phys. Rev. Lett. **81**, 5225 (1998).

[5] W. G. van der Wiel, S. D. Franceschi, T. Fujisawa, J. M. Elzerman, S. Tarucha, and L. P. Kouwenhoven, The Kondo effect in the unitary limit, Science **289**, 2105 (2000).

[6] Y. Nishida, SU(3) orbital Kondo effect with ultracold atoms, Phys. Rev. Lett. **111**, 135301 (2013).

[7] K. Ono, J. Kobayashi, Y. Amano, K. Sato, and Y. Takahashi, Antiferromagnetic interorbital spin-exchange interaction of ^{171}Yb, Phys. Rev. A **99**, 032707 (2019).

[8] L. Riegger, N. Darkwah Oppong, M. Höfer, D. R. Fernandes, I. Bloch, and S. Fölling, Localized magnetic moments with tunable spin exchange in a gas of ultracold fermions, Phys. Rev. Lett. **120**, 143601 (2018).

[9] S. Goto and I. Danshita, Quasiexact Kondo dynamics of fermionic alkaline-earth-like atoms at finite temperatures, Phys. Rev. Lett. **123**, 143002 (2019).

[10] K. Suzuki, S. Yasui, and K. Itakura, Interplay between chiral symmetry breaking and the QCD Kondo effect, Phys. Rev. D **96**, 114007 (2017).

[11] S. Yasui and S. Ozaki, Transport coefficients from the QCD Kondo effect, Phys. Rev. D **96**, 114027 (2017).

[12] P. Nozières, A "Fermi-liquid" description of the Kondo problem at low temperatures, J. Low Temp. Phys. **17**, 31 (1974).

[13] A. C. Hewson, Renormalized perturbation calculations for the single-impurity Anderson model, J. Phys.: Condens. Matter **13**, 10011 (2001).

[14] M. Grobis, I. G. Rau, R. M. Potok, H. Shtrikman, and D. Goldhaber-Gordon, Universal scaling in nonequilibrium transport through a single channel Kondo dot, Phys. Rev. Lett. **100**, 246601 (2008).

[15] G. D. Scott, Z. K. Keane, J. W. Ciszek, J. M. Tour, and D. Natelson, Universal scaling of nonequilibrium transport in the Kondo regime of single molecule devices, Phys. Rev. B **79**, 165413 (2009).

[16] A. V. Kretinin, H. Shtrikman, D. Goldhaber-Gordon, M. Hanl, A. Weichselbaum, J. von Delft, T. Costi, and D. Mahalu, Spin-$\frac{1}{2}$ Kondo effect in an InAs nanowire quantum dot: Unitary limit, conductance scaling, and Zeeman splitting, Phys. Rev. B **84**, 245316 (2011).

[17] A. V. Kretinin, H. Shtrikman, and D. Mahalu, Universal line shape of the Kondo zero-bias anomaly in a quantum dot, Phys. Rev. B **85**, 201301(R) (2012).

[18] M. Ferrier, T. Arakawa, T. Hata, R. Fujiwara, R. Delagrange, R. Weil, R. Deblock, R. Sakano, A. Oguri, and K. Kobayashi, Universality of non-equilibrium fluctuations in strongly correlated quantum liquids, Nat. Phys. **12**, 230 (2016).

[19] M. Ferrier, T. Arakawa, T. Hata, R. Fujiwara, R. Delagrange, R. Deblock, Y. Teratani, R. Sakano, A. Oguri, and K. Kobayashi, Quantum fluctuations along symmetry crossover in a Kondo-correlated quantum dot, Phys. Rev. Lett. **118**, 196803 (2017).

[20] T. Hata, Y. Teratani, T. Arakawa, S. Lee, M. Ferrier, R. Deblock, R. Sakano, A. Oguri, and K. Kobayashi, Three-body correlations in nonlinear response of correlated quantum liquid, Nat. Commun. **12**, 3233 (2021).

[21] C. Hsu, T. A. Costi, D. Vogel, C. Wegeberg, M. Mayor, H. S. J. van der Zant, and P. Gehring, Magnetic-field universality of the Kondo effect revealed by thermocurrent spectroscopy, Phys. Rev. Lett. **128**, 147701 (2022).

[22] C. Buizert, A. Oiwa, K. Shibata, K. Hirakawa, and S. Tarucha, Kondo universal scaling for a quantum dot coupled to superconducting leads, Phys. Rev. Lett. **99**, 136806 (2007).

[23] R. S. Deacon, Y. Tanaka, A. Oiwa, R. Sakano, K. Yoshida, K. Shibata, K. Hirakawa, and S. Tarucha, Tunneling spectroscopy of Andreev energy levels in a quantum dot coupled to a superconductor, Phys. Rev. Lett. **104**, 076805 (2010).

[24] R. S. Deacon, Y. Tanaka, A. Oiwa, R. Sakano, K. Yoshida, K. Shibata, K. Hirakawa, and S. Tarucha, Kondo-enhanced Andreev transport in single self-assembled InAs quantum dots contacted with normal and superconducting leads, Phys. Rev. B **81**, 121308(R) (2010).

[25] T. Hata, R. Delagrange, T. Arakawa, S. Lee, R. Deblock, H. Bouchiat, K. Kobayashi, and M. Ferrier, Enhanced shot noise of multiple Andreev reflections in a carbon nanotube quantum dot in SU(2) and SU(4) Kondo regimes, Phys. Rev. Lett. **121**, 247703 (2018).

[26] Y. Kanai, R. S. Deacon, S. Takahashi, A. Oiwa, K. Yoshida, K. Shibata, K. Hirakawa, Y. Tokura, and S. Tarucha, Electrically tuned spin–orbit interaction in an InAs self-assembled quantum dot, Nat. Nanotechnol. **6**, 511 (2011).

[27] D. M. Schröer, A. K. Hüttel, K. Eberl, S. Ludwig, M. N. Kiselev, and B. L. Altshuler, Kondo effect in a one-electron double quantum dot: Oscillations of the Kondo current in a weak magnetic field, Phys. Rev. B **74**, 233301 (2006).

[28] F. Bauer, J. Heyder, E. Schubert, D. Borowsky, D. Taubert, B. Bruognolo, D. Schuh, W. Wegscheider, J. von Delft, and S. Ludwig, Microscopic origin of the "0.7-anomaly" in quantum point contacts, Nature (London) **501**, 73 (2013).

[29] M. Žonda, O. Stetsovych, R. Korytár, M. Ternes, R. Temirov, A. Raccanelli, F. S. Tautz, P. Jelínek, T. Novotný, and M. Švec, Resolving ambiguity of the Kondo temperature determination in mechanically tunable single-molecule Kondo systems, J. Phys. Chem. Lett. **12**, 6320 (2021).

[30] A. Okiji and N. Kawakami, Magnetic properties of Anderson model at zero temperature, J. Phys. Soc. Jpn. **51**, 3192 (1982).

[31] N. Kawakami and A. Okiji, Low temperature thermodynamics of asymmetric Anderson model, J. Phys. Soc. Jpn. **52**, 1119 (1983).

[32] T. A. Costi, Magnetotransport through a strongly interacting quantum dot, Phys. Rev. B **64**, 241310(R) (2001).

[33] R. M. Konik, H. Saleur, and A. Ludwig, Transport in quantum dots from the integrability of the Anderson model, Phys. Rev. B **66**, 125304 (2002).

[34] M. Pustilnik and L. Glazman, Kondo effect in quantum dots, J. Phys.: Condens. Matter **16**, R513 (2004).

[35] T. S. Jespersen, M. Aagesen, C. Sørensen, P. E. Lindelof, and J. Nygård, Kondo physics in tunable semiconductor nanowire quantum dots, Phys. Rev. B **74**, 233304 (2006).

[36] L. Merker, S. Kirchner, E. Muñoz, and T. A. Costi, Conductance scaling in Kondo-correlated quantum dots: Role of level asymmetry and charging energy, Phys. Rev. B **87**, 165132 (2013).

[37] M. Filippone, C. P. Moca, A. Weichselbaum, J. von Delft, and C. Mora, At which magnetic field, exactly, does the Kondo resonance begin to split? A fermi liquid description of the low-energy properties of the Anderson model, Phys. Rev. B **98**, 075404 (2018).

[38] A. Oguri and A. C. Hewson, Higher-order fermi-liquid corrections for an Anderson impurity away from half filling, Phys. Rev. Lett. **120**, 126802 (2018).

[39] A. Oguri and A. C. Hewson, Higher-order Fermi-liquid corrections for an Anderson impurity away from half filling: Nonequilibrium transport, Phys. Rev. B **97**, 035435 (2018).

[40] Y. Teratani, R. Sakano, and A. Oguri, Fermi liquid theory for nonlinear transport through a multilevel Anderson impurity, Phys. Rev. Lett. **125**, 216801 (2020).

[41] A. Oguri, Y. Teratani, K. Tsutsumi, and R. Sakano, Current noise and Keldysh vertex function of an Anderson impurity in the Fermi-liquid regime, Phys. Rev. B **105**, 115409 (2022).

[42] N. Andrei, K. Furuya, and J. H. Lowenstein, Solution of the Kondo problem, Rev. Mod. Phys. **55**, 331 (1983).

[43] E. A. Laird, F. Kuemmeth, G. A. Steele, K. Grove-Rasmussen, J. Nygård, K. Flensberg, and L. P. Kouwenhoven, Quantum transport in carbon nanotubes, Rev. Mod. Phys. **87**, 703 (2015).

[44] K. Tsutsumi, Y. Teratani, R. Sakano, and A. Oguri, Nonlinear Fermi liquid transport through a quantum dot in asymmetric tunnel junctions, Phys. Rev. B **104**, 235147 (2021).

[45] J. R. Schrieffer and P. A. Wolff, Relation between the Anderson and Kondo Hamiltonians, Phys. Rev. **149**, 491 (1966).

[46] F. D. M. Haldane, Scaling theory of the asymmetric Anderson model, Phys. Rev. Lett. **40**, 416 (1978).